International Journal of Infrared and Millimeter Waves, Vol. 27, No. 1, January 2006 (© 2006)
DOI: 10.1007/s10762-006-9081-z

AN ANALYTICAL APPROACH ON THE DETERMINATION OF GENERATOR REFLECTION COEFFICIENTS USED IN THE NOISE-PARAMETER MEASUREMENT

Robert Hu and Tzu-Hsien Sang

Department of Electronics Engineering
National Chiao Tung University
Hsin-Chu, Taiwan R.O.C.

Received 5 September 2005

Abstract

In performing microwave and millimeter-wave noise-parameter measurements, a set of generator reflection coefficients and their corresponding noise temperatures need to be measured first. Allowing measurement errors, values of these generator reflection coefficients will affect the accuracy of final results. Though simulation alone can be used to find out on the Smith chart the preferred pattern of the generator reflection coefficients, its analytical counterpart has not been explored yet. This paper intends to derive the related mathematical expressions, thus complements and strengthens the simulation method.

Keywords: Generator reflection coefficient, noise parameters, noise temperature, least-squares fit.

1. Introduction

In the design of microwave and millimeter-wave low-noise amplifiers, both the small-signal model and noise model of the constituting transistors need to be known so they can be imported into the circuit simulators [1]–[6]. Compared with its small-signal model, the transistor's noise model is more difficult to construct, for it demands accurate measurements of the sensitive, and thus elusive, noise parameters, which in turn impose some stringent requirements on the noise measurement setup [7]–[14]. Of the many expressions for a two-port circuit's noise parameters, it is the minimum noise temperature T_{min}, noise ratio N, and optimum reflection coefficient Γ_{opt} (= $\gamma_{opt}\exp(j\,\theta_{opt})$), which is a complex number, that will be used in this paper. The relation between the noise

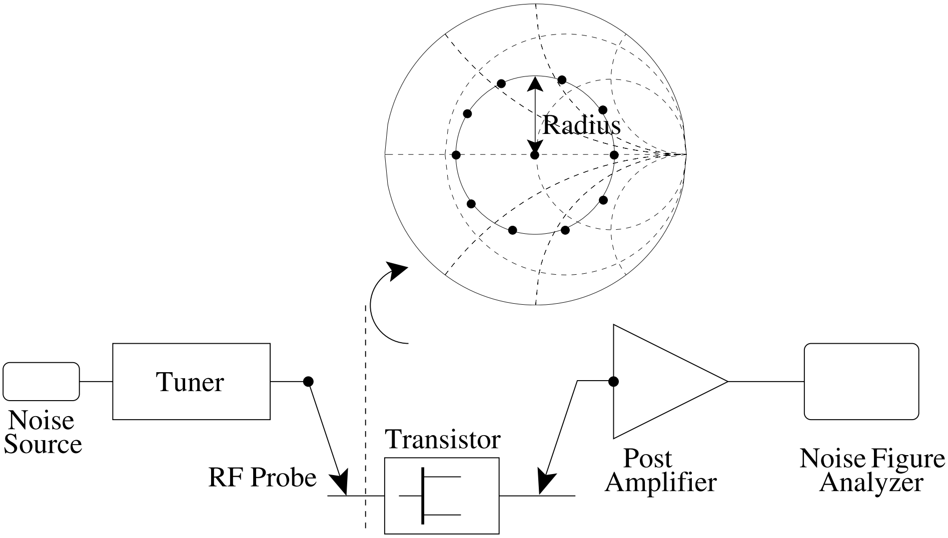

Fig. 1. Generator reflection coefficients used for noise-parameter measurement where the Γ_g pattern contains the zero point and a circle.

temperature and the noise parameters is

$$T_n = T_{min} + 4\,T_0\,N\,\frac{|\Gamma_g - \Gamma_{opt}|^2}{(1-|\Gamma_g|^2)\,(1-|\Gamma_{opt}|^2)} \qquad (1)$$

where T_o is 290 Kelvin, Γ_g (= $\gamma_g \exp(j\,\theta_g)$) is the generator reflection coefficient. Mathematically, the unknown noise parameters can be derived using least-squares fit from a set of generator reflection coefficients and their corresponding noise temperatures [15]–[19].

However, the choice of the Γ_g set cannot be arbitrary as some may cause the following noise calculation to be divergent, as in the case of a circular Γ_g on the Smith chart. While it is also known that the mere addition of the zero point, i.e., $\Gamma_g = 0$, into the above circular pattern results in the intended solutions (see Fig. 1). Moreover, when measurement uncertainty, or error, is taken into account, simulation shows that this Γ_g circle is preferred having a large radius if the uncertainty is embedded in the measured T_n, which is usually the case when measuring an ultra-sensitive transistor. Though it is convenient using the simulation approach to both determine the desired generator reflection coefficients and make an evaluation of different computation algorithms [20]–[23], this empirical approach cannot reveal much about the underlying physics, nor explains why the desired results can be rendered. In this paper, we intend to demonstrate that, through mathematical reasonings, several interesting conclusions can indeed be obtained without the running of numerous and laborious

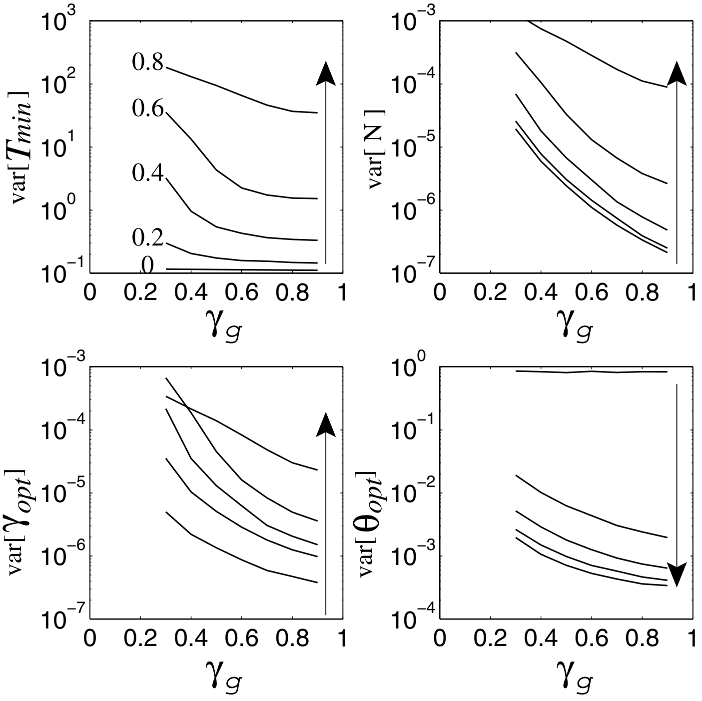

Fig. 2. Error analysis on the determination of generator reflection coefficients. The five curves in each subplot correspond to different values of Γ_{opt}.

simulations. In developing this analytical approach, better insight into the noise-parameter measurement can also be gained.

2. On the Choice of Γ_g

In this paper, the transistor, as the device under test, has its measured noise temperature embedded with uncertainty described by a Gaussian distribution with 5% standard deviation; on the Smith chart, the generator reflection coefficients contains the zero point and a circle. With different radius for the Γ_g circle, simulation reveals a preference for large radius, no matter Γ_{opt} is zero or not. Fig. 2 shows the error analysis on the noise parameters of the transistor that has T_{min} = 30 Kelvin, N = 0.035, and Γ_{opt} changing from 0 and 0.8. Subplots (a), (b), (c), (d) are the variance of T_{min}, N, γ_{opt} and θ_{opt}, with the radius of the Γ_g circle on the X-axis. In each subplot, the five curves correspond to optimum reflection coefficient of 0, 0.2, 0.4, 0.6 and 0.8 respectively, with the direction of increasing Γ_g indicated by the arrow. This large-radius preference also holds when certain T_n-dependent weighting factor is included in the simulation.

To begin the formulation, the nonlinear noise temperature expression of Eq. 1 has to be re-arranged as a linear function of four new variables a, b, c and d:

$$T_n = a + b\,\frac{1}{1-\gamma_g^2} + c\,\frac{\gamma_g\,\cos(\theta_g)}{1-\gamma_g^2} + d\,\frac{\gamma_g\,\sin(\theta_g)}{1-\gamma_g^2} \tag{2}$$

with

$$\begin{aligned} a &= -4\,T_0\,N\,\frac{1}{1-\gamma_{opt}^2} + T_{min} \\ b &= \quad 4\,T_0\,N\,\frac{1+\gamma_{opt}^2}{1-\gamma_{opt}^2} \\ c &= -8\,T_0\,N\,\frac{\gamma_{opt}\,\cos(\theta_{opt})}{1-\gamma_{opt}^2} \\ d &= -8\,T_0\,N\,\frac{\gamma_{opt}\,\sin(\theta_{opt})}{1-\gamma_{opt}^2}\,. \end{aligned} \tag{3}$$

By setting $\Delta = \sqrt{b^2 - c^2 - d^2}$, we also have

$$\begin{aligned} T_{min} &= a + \frac{b+\Delta}{2} \\ N &= \frac{\Delta}{4\,T_0} \\ \gamma_{opt} &= \sqrt{\frac{b-\Delta}{b+\Delta}} \\ \theta_{opt} &= \tan^{-1}(\frac{d}{c})\,. \end{aligned} \tag{4}$$

At each frequency point, the set of different generator reflection coefficients Γ_i (= $\gamma_i \exp{(j\,\theta_i)}$) and their corresponding noise temperatures T_i, with $i = 1 \sim m$, can be arranged as

$$\begin{bmatrix} T_1 \\ T_2 \\ \vdots \\ T_m \end{bmatrix} = \begin{bmatrix} 1 & \frac{1}{1-\gamma_1^2} & \frac{\gamma_1\,\cos(\theta_1)}{1-\gamma_1^2} & \frac{\gamma_1\,\sin(\theta_1)}{1-\gamma_1^2} \\ 1 & \frac{1}{1-\gamma_2^2} & \frac{\gamma_2\,\cos(\theta_2)}{1-\gamma_2^2} & \frac{\gamma_2\,\sin(\theta_2)}{1-\gamma_2^2} \\ \vdots & \vdots & \vdots & \vdots \\ 1 & \frac{1}{1-\gamma_m^2} & \frac{\gamma_m\,\cos(\theta_m)}{1-\gamma_m^2} & \frac{\gamma_m\,\sin(\theta_m)}{1-\gamma_m^2} \end{bmatrix} \begin{bmatrix} a \\ b \\ c \\ d \end{bmatrix} \tag{5}$$

or in a more concise matrix form

$$[T] = [X]\;[A]\;. \tag{6}$$

Applying the least-squares fit, there is

$$[A] = ([X]^t\,[X])^{-1}\,[X]^t\,[T]\,. \tag{7}$$

hus a, b, c, d and the four noise parameters at this frequency point can be obtained if the generator reflection coefficients and their related noise temperatures are known.

If there is uncertainty embedded in the noise temperature, the resulting noise parameters will show some deviation from their ideal values. By assuming the uncertainty Gaussian, error-analysis simulation can be employed figuring out the variance for each noise parameter. Indeed, the simulated results confirm the large-radius preference for the Γ_g circle. However, simulation alone cannot explain why it works that way, nor whether the simulated results is valid for other circuits; all this demand a more analytical, and thus comprehensive, approach. First, with the optimum reflection coefficient set to zero, the difference between mismatched and matched noise temperatures is

$$\triangle T_n = b\,\frac{\gamma_g^2}{1-\gamma_g^2} + c\,\frac{\gamma_g}{1-\gamma_g^2}\,\cos(\theta_g) + d\,\frac{\gamma_g}{1-\gamma_g^2}\,\sin(\theta_g)\,. \tag{8}$$

So if b, c and d are known, variable a and the original four noise parameters can be calculated from $\triangle T_n$. To simplify the derivation procedure, we let

$$B = b\,\frac{\gamma_g^2}{1-\gamma_g^2}\,; \quad C = c\,\frac{\gamma_g}{1-\gamma_g^2}\,; \quad D = d\,\frac{\gamma_g}{1-\gamma_g^2}\,. \tag{9}$$

Values of B, C and D can be determined using least-squares fit with error term ϵ^2 defined as

$$\epsilon^2 \equiv \frac{1}{m}\Sigma\left[B + C\cdot\cos(\theta_g) + D\cdot\sin(\theta_g) - \triangle T_n\right]^2\,. \tag{10}$$

Here the summation Σ includes all the m sampling points on the Γ_g circle. Since least-squares fit demands the partial differential of the error term versus variables B, C and D must be zero, i.e.

$$\frac{\partial\,\epsilon^2}{\partial\,B} = \frac{\partial\,\epsilon^2}{\partial\,C} = \frac{\partial\,\epsilon^2}{\partial D} = 0\,, \tag{11}$$

there will be

$$\begin{aligned}
&B\cdot\Sigma 1 + C\cdot\Sigma\cos(\theta_g) + D\cdot\Sigma\sin(\theta_g) = \Sigma\triangle T_n\\
&B\cdot\Sigma\cos(\theta_g) + C\cdot\Sigma\cos^2(\theta_g) + D\cdot\Sigma\sin(\theta_g)\cos(\theta_g) = \Sigma\triangle T_n\cos(\theta_g)\\
&B\cdot\Sigma\sin(\theta_g) + C\cdot\Sigma\cos(\theta_g)\sin(\theta_g) + D\cdot\Sigma\sin^2(\theta_g) = \Sigma\triangle T_n\sin(\theta_g)\,.
\end{aligned} \tag{12}$$

With a suitable sampling scheme, it is reasonable assuming the following hold:

$$\Sigma\sin(\theta_g) = \Sigma\cos(\theta_g) = \Sigma\sin(\theta_g)\cos(\theta_g) \approx 0\,. \tag{13}$$

Eq. 12 can thus be re-arranged as

$$\begin{bmatrix} m & 0 & 0\\ 0 & \Sigma\cos^2(\theta_g) & 0\\ 0 & 0 & \Sigma\sin^2(\theta_g)\end{bmatrix}\begin{bmatrix} B\\ C\\ D\end{bmatrix} = \begin{bmatrix}\Sigma\triangle T_n\\ \Sigma\triangle T_n\cos(\theta_g)\\ \Sigma\triangle T_n\sin(\theta_g)\end{bmatrix}. \tag{14}$$

Variables B, C, D and therefore b, c, d can be easily obtained:

$$\begin{aligned} b &= \frac{1-\gamma_g^2}{\gamma_g}\frac{1}{m}\Sigma\left[\Delta T_n\right] \\ c &= \frac{1-\gamma_g^2}{\gamma_g}\frac{1}{m}\Sigma\left[\Delta T_n\cdot\cos(\theta_g)\right] \\ d &= \frac{1-\gamma_g^2}{\gamma_g}\frac{1}{m}\Sigma\left[\Delta T_n\cdot\sin(\theta_g)\right]\ . \end{aligned} \tag{15}$$

If there is no measurement uncertainty, we will have

$$b = 4\,T_0\,N\,; \qquad c = 0\,; \qquad d = 0\,, \tag{16}$$

which are their original values. If the uncertainty has finite value and is proportional to the measured noise temperature, then

$$\begin{aligned} \triangle T_n &= (1+\delta_1)\,T_n^{mismatched} - (1+\delta_2)\,T_n^{matched} \\ &= (1+\delta_1)\left(T_{min} + 4\,T_0\,N\,\frac{\gamma_g^2}{1-\gamma_g^2}\right) - (1+\delta_2)\,T_{min} \end{aligned} \tag{17}$$

where δ_1 and δ_2 represent the uncertainty values for the mismatched and matched noise temperatures. Neglecting their respective higher-order terms, uncertainty values of the four noise variables will be

$$\begin{aligned} \Delta a &= -\,\frac{1-\gamma_g^2}{\gamma_g^2}T_{min}\frac{1}{m}\sum\delta_1 - 4\,T_0\,N\frac{1}{m}\sum\delta_1 + \frac{1}{\gamma_g^2}T_{min}\frac{1}{m}\sum\delta_2 \\ \Delta b &= 4\,T_0\,N\frac{1}{m}\Sigma\,\delta_1 + \frac{1-\gamma_g^2}{\gamma_g^2}\,T_{min}\frac{1}{m}\Sigma\,(\delta_1-\delta_2) \\ \Delta c &= 8\,T_0\,N\,\gamma_g\frac{1}{m}\Sigma\left[\delta_1\cdot\cos(\theta_g)\right] + 2\,T_{min}\,\frac{1-\gamma_g^2}{\gamma_g}\frac{1}{m}\Sigma\left[(\delta_1-\delta_2)\cdot\cos(\theta_g)\right] \\ \Delta d &= 8\,T_0\,N\,\gamma_g\frac{1}{m}\Sigma\left[\delta_1\cdot\sin(\theta_g)\right] + 2\,T_{min}\,\frac{1-\gamma_g^2}{\gamma_g}\frac{1}{m}\Sigma\left[(\delta_1-\delta_2)\cdot\sin(\theta_g)\right]\ . \end{aligned} \tag{18}$$

If δ_1 and δ_2 are slowly-drifting functions with

$$\begin{aligned} 0 &= \Sigma\left[\delta_1\cdot\cos(\theta_g)\right] = \Sigma\left[(\delta_1-\delta_2)\cdot\cos(\theta_g)\right] \\ &= \Sigma\left[\delta_1\cdot\sin(\theta_g)\right] = \Sigma\left[(\delta_1-\delta_2)\cdot\sin(\theta_g)\right]\ , \end{aligned} \tag{19}$$

then both Δc and Δd turn to be zero. A large γ_g in this case reduces the derived Δa and Δb, thus results in more precise solutions for the noise parameters. If both δ_1 and δ_2 are uncorrelated random variables with

$$var\left[\frac{1}{m}\Sigma\delta_1\right] = \sigma_1^2\,; \qquad var\left[\frac{1}{m}\Sigma\delta_2\right] = \sigma_2^2 \tag{20}$$

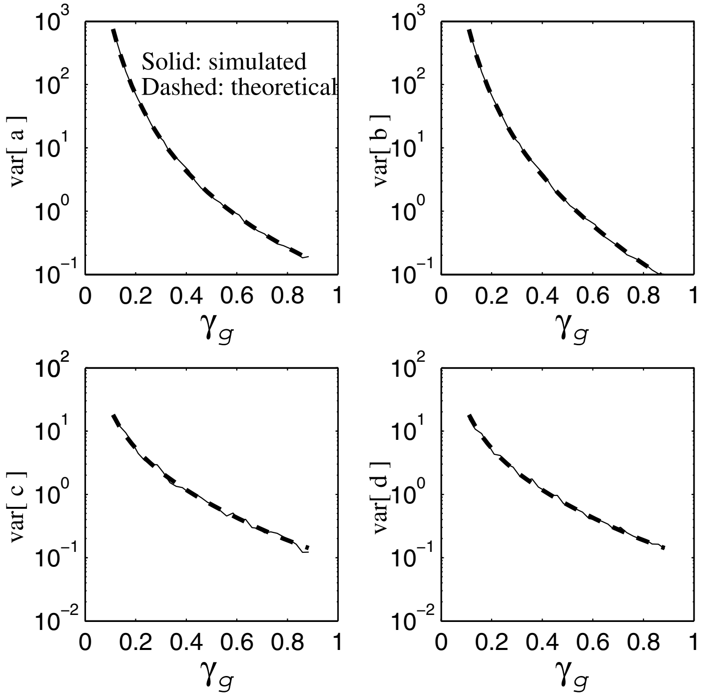

Fig. 3. Error analysis on the four noise variables. With 100 simulation runs, the variance of the simulated noise variables using least-squares fit agree with their theoretical counterparts.

where $var[\cdots]$ is the statistical variation function, then Eq. 18 leads to

$$\begin{aligned} var\,[\,a\,] &= \sigma_1^2 \left(\frac{1-\gamma_g^2}{\gamma_g^2}\, T_{min} + 4\,T_0\,N \right)^2 + \sigma_2^2 \left(\frac{1}{\gamma_g^2}\, T_{min} \right)^2 \\ var\,[\,b\,] &= \sigma_1^2 \left(\frac{1-\gamma_g^2}{\gamma_g^2}\, T_{min} + 4\,T_0\,N \right)^2 + \sigma_2^2 \left(\frac{1-\gamma_g^2}{\gamma_g^2}\, T_{min} \right)^2 \\ var\,[\,c\,] &= var\,[\,d\,] = 2\,\sigma_1^2 \left(\frac{1-\gamma_g^2}{\gamma_g^2}\, T_{min} \right)^2 + \sigma_2^2 \left(\frac{1-\gamma_g^2}{\gamma_g^2}\, T_{min} \right)^2 . \end{aligned} \tag{21}$$

All these four expressions show that, in order to minimize the variation, the radius of the Γ_g circle needs to be large. Accuracy of Eq. 21 can be easily confirmed through simulation, as in Fig. 3. Here the error analysis on the four new noise parameters is carried out assuming 5% Gaussian uncertainty on the measured noise temperatures, and 100 simulation runs are used for averaging.

Subplots (a), (b), (c), (d) show the variance of a, b, c and d, with X-axis the radius of the Γ_g circle. In each subplot, the solid curve is the simulated result with noise parameters derived from Eq. 7, and the optimum reflection coefficient is assumed zero; the dashed curve is its theoretical counterpart calculated directly from Eq. 21. Agreement between the solid and dashed curves in each subplot substantiates our mathematical work. Of course, if we reduce the number of simulations from 100 to 10, then there will be noticeable discrepancy between the simulated variance of the noise variable and its theoretical counterpart.

3. Discussion on the Mathematical Implications

Though the derivation in the previous section is done by assuming zero Γ_{opt} to reduce the mathematical complexity, the impact of non-zero Γ_{opt} can be understood by applying the sensitivity analysis on the least-squared solutions [24]. In the case of non-zero Γ_{opt}, Eq. 14 needs to be revised as

$$\begin{aligned}\left(\begin{bmatrix} m & 0 & 0 \\ 0 & \Sigma\cos^2(\theta_g) & 0 \\ 0 & 0 & \Sigma\sin^2(\theta_g) \end{bmatrix} + \Delta_F\right)\begin{bmatrix} B \\ C \\ D \end{bmatrix} \\ = \left(\begin{bmatrix} \Sigma\triangle T_n \\ \Sigma\triangle T_n\cos(\theta_g) \\ \Sigma\triangle T_n\sin(\theta_g) \end{bmatrix} + \Delta_f\right).\end{aligned} \tag{22}$$

where Δ_F and Δ_f are the perturbation matrices consisted of terms with magnitude at the order of $[(1-\gamma_g^2)/\gamma_g]\cdot[\gamma_{opt}/(1-\gamma_{opt}^2)]$. Two observations emerge from this perturbation expression. First, the effect of a non-zero Γ_{opt} is quite limited if γ_{opt} is small. Second, a large γ_g helps reducing the impact of non-zero γ_{opt}. The latter is because the condition number of a matrix indicates its solution's sensitivity to perturbation [25], and in our case the diagonal matrix has a small condition number–close to 2, which implies a low sensitivity. It is this property that explains why a non-zero Γ_{opt} will not alter the general trend that large generator reflection coefficients are preferred in deriving the noise parameters using least-squares fit.

As in other fields [26], sometimes it is the analytical approach that offers solutions to some peculiar phenomena. For example, in order to explain the seemingly anomalous T_{min} variance, i.e., a straight line versus Γ_g when Γ_{opt} is zero (see Fig. 2), it is the knowledge of explicit expressions for the variance of a, b, c and d that helps. Since there is from Eq. 4

$$T_{min} = a + \frac{b + \sqrt{b^2 - c^2 - d^2}}{2}. \tag{23}$$

With the mean values of c and d now zero and their variance one order less than that of a and b, the variance of T_{min} can be approximated as

$$var\,[\,T_{min}\,] = var\,[\,a + b\,] = \sigma_2^2\,T_{min}^2\,, \tag{24}$$

which, apparently, is independent of γ_g. Thus, the choice of the generator reflection coefficient has negligible impact on the minimum noise temperature when the optimum reflection coefficient is zero.

Finally, we would like to consider other uncertainty modelings. To be sure, there are two possible sources of uncertainty in the noise-parameter measurement, one is on the noise temperature itself and the other on the generator reflection coefficient. Our approach is to focus on T_n uncertainty while assuming a perfect measurement of Γ_g. Some authors, however, emphasize the benefits of considering simultaneously both uncertainty sources [27]-[31]. While it is true that by doing so the accuracy of the simulated results can be improved, it will not change the main conclusion of this paper, that is, the radius of the Γ_g circle should be as large as possible in order to minimize the impact of the measurement fluctuation. This is because if the relation between T_n and γ_g is a smooth and monotonic function, it is always possible merging the two uncertainty sources into one, for the reason that in this case the Gaussian uncertainty in one quantity can be approximately mapped into the other quantity as Gaussian, and vice versa. As long as it is the small variation involved, leaving out one uncertainty while keeping the other one will not cause problems [32]-[34].

4. Conclusion

In this paper, an analytical approach on the determination of generator reflection coefficients used in the noise-parameter measurement has been developed. The reason why a large generator reflection coefficient is preferred in the noise measurement is now soundly explained. Agreements between the mathematical expressions and their simulation counterparts have also been checked.

Acknowledgments

Author R. Hu would like to thank S. Weinreb, D. Miller, J. Kooi, M. Edgar, F. Rice, G. Chattopadhyay and Prof. J. Zmuidzinas of Caltech, Pasadena, for discussions and encouragement.

References

[1] R. Hu, “An 8–20-GHz wide-band LNA design and the analysis of its input matching mechanism,” *IEEE Microwave Wireless Comp. Lett.*, vol. 14, pp. 528-530, Nov. 2004.

[2] R. Hu, M.S. Yang, “Investigation of different input-matching mechanisms used in wide-band LNA design,” *Intl. J. IR & MM Waves*, vol. 26, pp. 221-245, Feb. 2005.

[3] A. Pascht, M. Grozing, D. Weigner, M. Berroth, "Small-signal and temperature noise model for MOSFETs," *IEEE Trans. Microwave Theory Tech.,* vol. 50, pp. 1927–1934, Aug. 2002.

[4] A. Casmi, B. Huyart, E. Bergeault, L. P. Jallet, "Small-signal and temperature noise model for MOSFETs," *IEEE Trans. Microwave Theory Tech.,* vol. 50, pp. 1927–1934, Aug. 2002.

[5] H. Fukui, "Design of microwave GaAs MESFET's for broad-band low-noise amplifiers," *IEEE Trans. Microwave Theory Tech.,* vol. 27, pp. 643–650, July 1979.

[6] M. R. Murti, J. Laskar, S. Nuttinck, Y. Yoo, A. Raghaven, J. I. Bergman, J. Bautista, R. Lai, F. Grundbacher, M. Barsky, P. Chin, P. H. Liu, "temperature dependent small signal and noise parameter measurements and modeling on InP HEMTs," *IEEE Trans. Microwave Theory Tech.,* vol. 48, pp. 2579–2587, Dec. 2000.

[7] T. Vaha-Heikkila, M. Lahdes, M. Kantanen, J. Tuovinen, "On-wafer noise-parameter measurements at W-band," *IEEE Trans. Microwave Theory Tech.,* vol. 51, pp. 1621–1627, June 2003.

[8] M. Kantanen, M. Lahdes, T. Vaha-Heikkila, J. Tuovinen, "A wide-band on-wafer noise-parameter measurement system at 50–75 GHz," *IEEE Trans. Microwave Theory Tech.,* vol. 51, pp. 1489–1495, May 2003.

[9] R. Hu, S. Weinreb, "A novel wide-band noise-parameter measurement method and its cryogenic application," *IEEE Trans. Microwave Theory Tech.,* vol. 52, pp. 1498–1507, May 2004.

[10] R. Hu, T. H. Sang, "On-wafer noise parameter measurements using wide-band frequency variation method," *IEEE Trans. Microwave Theory Tech.,* vol. 53, pp. 2398–2402, July 2005.

[11] E. C. Valk, D. Rutledge, J. F. Vaneldik, T. L. Landecker, "De-embedding two-port noise parameters using a noise wave model," *IEEE Trans. Microwave Theory Tech.,* vol. 37, pp. 195–200, June 1988.

[12] A. Caddemi, A. Di Paola, M. Sannino, "Determination of HEMTs noise parameters versus temperature using two measurement methods," *IEEE Trans. Microwave Theory Tech.,* vol. 47, pp. 6–10, Feb. 1998.

[13] T. A. Alam, R. D. Rollard, C. M. Snowden, "Determination of W-band noise parameters," *Electronics Letters,* vol. 34, pp. 288–289, Feb. 1998.

[14] A. Boudiaf, M. Laporte, "An accurate and repeatable technique for noise parameter measurements," *IEEE Trans. Instrum. Meas.,* vol. 42, pp. 532–537, Apr. 1993.

[15] L. Escotte, J. G. Tartarin, J. Graffeuil, "A cost-effective technique for extending the low-frequency range of a microwave noise parameter test," *IEEE Trans. Instrum. and Meas.,* vol. 48, pp. 830–834, Aug. 1999.

[16] G. Niu, J. D. Cressier, S. Zhang, W. E. Ansley, C. S. Webster, D. L. Harame, "A unified approach to RF and microwave noise parameter modeling in bipolar transistors," *IEEE Trans. Electron Device,* vol. 48, pp. 2568–2574, Nov. 2001.

[17] J. Gao, C. L. Law, H. Wang, S. Aditya, G. Boeck, "A new method for pHEMT noise parameter determination based on 50Ω noise measurement system," *IEEE Trans. Microwave Theory Tech.,* vol. 51, pp. 2079–2089, Oct. 2003.

[18] C. E. Mcintosh, R. D. Pollard, R. E. Miles, "On the feasibility of using an active tuner for measuring microwave noise parameters," *IEEE Trans. Instrum. and Meas.,* vol. 48, pp. 1294–1300, Dec. 1999.

[19] M. S. Gupta, P. T. Greiling, "Microwave noise characterization of GaAs MESFET's: determination of extrinsic noise parameters," *IEEE Trans. Microwave Theory Tech.,* vol. 36, pp. 745–751, Apr. 1988.

[20] S. Van den Bosch, L, Martens, "Experimental verification of pattern selection for noise characterization," *IEEE Trans. Microwave Theory Tech.,* vol. 48, pp. 156–158, Jan. 2000.

[21] A. C. Davison, B. W. Leake, E. Strid, "Accuracy improvements in microwave noise parameter measurements," *IEEE Trans. Microwave Theory Tech.,* vol. 37, pp. 1973–1978, Dec. 1989.

[22] L. Escotte, R. Plana, J. Graffeuil, "Evaluation of Noise Parameter Extraction Methods," *IEEE Trans. Microwave Theory Tech.,* vol. 41, pp. 382–387, March 1993.

[23] A. Boudiaf, C. Dubon-Chevallier, D. Pasquet, "Verification of on-wafer noise parameter measurements," *IEEE Trans. Instrum. and Meas.,* vol. 44, pp. 332–335, Apr. 1995.

[24] L. H. Golub, C. F. Van Loan, "Matrix Computations," *The Johns Hopkins University Press,* 1996.

[25] N. J. Higham, "Accuracy and Stability of Numerical Algorithms," *SIAM Publications,* 1996.

[26] W. P. Zhu, M. O. Ahmad, M. Swamy, "An analytical approach for obtaining a closed-form solution to the least-square design problem of 2-D zero-phase FIR filters," *IEEE Trans. Circuits and Syst. II,* . vol. 41, pp. 796–807, Dec. 1994.

[27] T. Abatzoglou, J. Mendel, “Constrained total least squares,” *IEEE international conference on acoustics, speech, and signal processing, ICASSP '87* vol. 12, pp. 1485–1488, Apr. 1987.

[28] J. A. Cadzow, D. M. Wilkes, “Constrained total least squares: signal and system modeling,” *IEEE international conference on acoustics, speech, and signal processing, ICASSP-92,* vol. 5, pp. 277–280, March 1992

[29] P. D. Fiore, G. C. Verghese, “Constrained maximum likelihood solution of linear equations,” *IEEE Trans. Signal Processing,* vol. 48, pp. 671–679, March 2000.

[30] G. D’Antona, “The full least-squares method,” *IEEE Trans. Instrum. Meas.,* vol. 52, pp. 189–196, Feb. 2003.

[31] A. Sabharwal, L. G. Potter, “Convexly constrained linear inverse problems: iterative least-squares and regularization,” *IEEE Trans. Signal Processing,* vol. 46, pp. 2345–2356, Sep. 1998.

[32] B. De Moor, J. Vandewalle, “A unifying theorem for linear and total linear least squares,” *, IEEE Trans. Automat. Contr.,* vol. 35, pp. 563–566, May, 1990.

[33] E. M. Dowling, R. D. DeGroat, “The equivalence of the total least squares and minimum norm methods,” *IEEE Trans. Signal Processing,* vol. 39, pp. 1891–1892, Aug. 1991.

[34] P. Lemmerling, B. De Moor, S. Van Huffel, “On the equivalence of constrained total least squares and structured total least squares,” *IEEE Trans. Signal Processing,* vol. 44, pp. 2908–2911, Nov. 1996.